Screen-Printed NiS Thick Films for Efficient Gas Sensing Applications

Satishkumar Damodhar Thakare

Department of Chemistry, Karmaveer Ramraoji Aher Arts, Science and Commerce College, Deola, Tal-Deola, Dist. Nashik, State- Maharashtra, India

Abstract:
In the present study, NiS thick films were prepared by the screen-printing technique and investigated for gas sensing applications. The prepared NiS thick films were evaluated for their gas sensing response toward different gases, including LPG, NH_3, H_2S, C_2H_5OH, NO_2 and CH_4 at different operating temperatures. The gas sensing characteristics were found to be strongly dependent on the operating temperature and target gas. Among the investigated gases, the NiS thick film exhibited the highest response toward LPG (66.39%) at 120 °C, indicating its excellent suitability for LPG detection. The selectivity study revealed a maximum selectivity of 100% toward LPG, followed by NO_2 (62.77%), ethanol (38.68%), NH_3 (35.41%), H_2S (17.13%) and CH_4 (9.85%). The LPG concentration-dependent study demonstrated that the gas response increased from 46.58% at 100 ppm to a maximum of 66.39% at 500 ppm, followed by variations at higher concentrations. The dynamic sensing characteristics of the NiS thick film showed a response time of 23 s and recovery time of 78 s, demonstrating relatively rapid response and satisfactory recovery behavior. The observed sensing performance is attributed to the interaction of LPG molecules with chemisorbed oxygen species and active surface sites of the NiS thick film, resulting in changes in surface charge-carrier concentration and electrical resistance. The results demonstrate that screen-printed NiS thick films are promising sensing materials for selective LPG detection and gas-monitoring applications.

Keywords: NiS thick film; LPG sensing; gas response; selectivity; response time; recovery time; metal sulfide; gas detection.

I. Introduction

The rapid growth of industrialization, transportation, domestic fuel consumption and chemical-processing activities has resulted in increasing concerns regarding air pollution and the accidental release of combustible and toxic gases [1, 2]. Gases such as ammonia (NH_3), hydrogen sulfide (H_2S), nitrogen dioxide (NO_2), methane (CH_4), volatile organic compounds (VOCs) and liquefied petroleum gas (LPG) can adversely affect human health, environmental quality and industrial safety when present above permissible levels [3-5]. Therefore the development of reliable gas sensors capable of detecting hazardous and combustible gases with high response, good selectivity, rapid response/recovery, low cost and simple fabrication has become an important area of research. Semiconductor-based chemiresistive gas sensors are particularly attractive because gas adsorption at the sensing surface produces a measurable change in electrical resistance or conductance [6, 7]. The sensing performance is generally governed by parameters such as gas response, selectivity, operating temperature, response and recovery time, stability and detection range [6-8].

Metal-oxide semiconductors such as SnO_2, ZnO, TiO_2, WO_3, Fe_2O_3 and NiO have been extensively investigated as gas-sensing materials because of their chemical stability, surface activity and relatively simple fabrication. However, conventional metal-oxide sensors frequently require elevated operating temperatures

and may suffer from limitations associated with selectivity, power consumption and long-term stability [8-10]. These limitations have stimulated the exploration of alternative semiconductor materials, particularly metal sulfides. Metal sulfides possess tunable electronic structures, abundant surface-active sites and favorable surface chemistry, making them attractive candidates for gas-sensing applications [11, 12]. Nanostructured sulfides can provide a large surface-to-volume ratio and enhanced interaction with gas molecules, while their electronic properties can be modified through morphology control, defect engineering, doping, functionalization and heterostructure formation [12, 13].

Among various metal sulfides, nickel sulfide (NiS) is an interesting transition-metal sulfide because of its distinctive electrical, chemical and surface properties. NiS can exhibit different structural phases depending on preparation conditions, and its electronic characteristics make it suitable for applications in sensing, electrochemical devices, energy storage and catalysis [1, 5, 9]. From a gas-sensing perspective, the surface of NiS provides active sites for adsorption of atmospheric oxygen and target gas molecules. The interaction between adsorbed oxygen species and the incoming gas molecules modifies the surface charge-carrier concentration and consequently changes the electrical resistance of the sensing layer [11, 12]. Such surface-reaction-driven resistance variation forms the fundamental basis of chemiresistive gas sensing. In metal-sulfide sensors, gas adsorption, charge transfer and surface reaction processes strongly influence response magnitude, selectivity and recovery characteristics [13, 14].

LPG is of particular interest for gas-sensing studies because it is widely used as a domestic and industrial fuel. LPG generally consists primarily of hydrocarbons such as propane and butane and is highly combustible. Accidental leakage can result in fire, explosion and serious safety hazards, particularly in confined domestic and industrial environments [14, 15]. Therefore, rapid and reliable LPG detection is important for preventing accidents and improving fuel-handling safety. Thick-film semiconductor sensors have previously demonstrated their usefulness for LPG detection, including sensors fabricated using screen-printing technology [15, 16].

The screen-printing technique is particularly attractive for the fabrication of thick-film gas sensors because it is simple, economical, reproducible and suitable for large-area deposition. In this method, a prepared sensing paste is deposited onto an appropriate substrate through a patterned screen, followed by drying and thermal treatment to obtain a mechanically stable and electrically active sensing layer [17, 18]. The thickness, morphology and porosity of the resulting film can be controlled through paste composition, screen parameters, printing conditions and thermal treatment. The resulting thick-film structure can provide a large interaction area between the sensing material and target gas, while the fabrication method is compatible with relatively simple sensor architectures and scalable production. Previous studies have demonstrated the suitability of screen printing for thick-film gas sensors, including LPG and other gas-sensing systems. The choice of NiS in thick-film form is therefore of considerable interest because it combines the favorable surface chemistry of a metal sulfide with the practical advantages of thick-film fabrication. The gas-sensing performance of such a film can be evaluated by exposing it to different gases at controlled operating temperatures and concentrations and monitoring the corresponding electrical response [17-20].

In the present work, NiS thick films were fabricated using the screen-printing method and systematically investigated for gas-sensing applications. The sensing behavior was studied as a function of operating temperature toward LPG, NH_3, H_2S, C_2H_5OH, NO_2 and CH_4. Particular attention was given to the optimization of the operating temperature, comparative gas response, selectivity, LPG concentration-dependent response and dynamic response/recovery characteristics. The NiS thick film exhibited its maximum gas response of

66.39% toward LPG at 120 °C, while the selectivity investigation showed a maximum value of 100% for LPG. The LPG concentration study further demonstrated a maximum response of 66.39% at 500 ppm, and the dynamic sensing measurements yielded a response time of 23 s and recovery time of 78 s. These results demonstrate the potential of screen-printed NiS thick films as efficient sensing layers for LPG detection and provide a basis for their further development in domestic safety, industrial monitoring and environmental gas-sensing applications.

II. Material and Methods

A) Synthesis of NiS nanoparticles

NiS nanoparticles were synthesized by a simple chemical precipitation method using analytical-grade nickel chloride hexahydrate ($NiCl_2 \cdot 6H_2O$) and sodium sulfide nonahydrate ($Na_2S \cdot 9H_2O$) as starting materials. Initially, 2.376 g of $NiCl_2 \cdot 6H_2O$ was accurately weighed and dissolved in 100 mL of deionized water to prepare a 0.1 M nickel precursor solution. The solution was continuously stirred at 600 rpm for 30 min at room temperature to obtain a clear and homogeneous solution. Separately, 2.402 g of $Na_2S \cdot 9H_2O$ was dissolved in 100 mL of deionized water to prepare a 0.1 M sodium sulfide solution. The prepared sodium sulfide solution was then added slowly and dropwise to the nickel precursor solution under continuous magnetic stirring at 600 rpm. During the addition, the pH of the reaction mixture was maintained at approximately 10–11 using dilute NaOH solution. After complete addition, the reaction mixture was continuously stirred at 600 rpm for 4 h at room temperature (25–30 °C) to ensure complete precipitation and homogeneous formation of NiS nanoparticles [20, 21]. The resulting black precipitate was then allowed to age for approximately 12 h at room temperature. The precipitate was separated by filtration and washed several times with deionized water and ethanol to remove unreacted ions and soluble impurities. The washed precipitate was dried under an IR lamp at 80–100 °C for approximately 6 h. The dried material was subsequently ground using an agate mortar and pestle to obtain a fine powder. Finally, the obtained NiS powder was calcined at 300 °C for 2 h and allowed to cool naturally to room temperature. The calcined powder was again gently ground to obtain a fine and homogeneous NiS nanopowder, which was subsequently used for the preparation of the sensing paste and fabrication of NiS thick films by the screen-printing technique [8-11].

B) Preparation of NiS thick films using screen printing method

The synthesized NiS nanopowder was used to prepare NiS thick films by the screen-printing technique. Initially, the required amount of NiS nanopowder was finely ground using an agate mortar and pestle to obtain a uniform and homogeneous powder. The NiS powder was then mixed with a suitable organic vehicle to prepare a printable paste. A 70:30 weight ratio of NiS powder to organic vehicle was maintained to obtain appropriate viscosity and printability [10, 13]. The mixture was thoroughly homogenized for approximately 1–2 h to ensure uniform dispersion of NiS particles and to avoid agglomeration. A clean glass substrate was used for deposition and was initially washed with detergent and deionized water, followed by cleaning with ethanol and drying. A suitable screen-printing mesh was placed over the substrate, and the prepared NiS paste was spread uniformly over the screen using a squeegee with controlled pressure to obtain a homogeneous thick-film layer. The printed film was initially dried under an IR lamp for approximately 20–30 min to remove the organic solvent and improve adhesion of the deposited layer. Finally, the dried NiS thick films were subjected to thermal annealing at approximately 300 °C for 2–3 h to remove the remaining organic components, improve adhesion and enhance the structural stability and crystallinity of the NiS sensing layer [15].

III. Result and Discussion

Figure 1 illustrates the schematic arrangement and working principle of the gas-sensing system used to evaluate the sensing performance of the screen-printed NiS thick films. The system consists of a 25 L gas-testing chamber, a glass dome, NiS thick-film sensing element, heating arrangement, electrical measurement circuit, gas inlet and outlet ports, and a regulated power supply. The NiS thick film is mounted on a suitable base plate/substrate inside the glass dome, while a Pt coil heater is positioned beneath or close to the sensing element to provide controlled operating temperature [16-18]. The heater is supplied with 230 V AC, and the operating temperature of the sensing film is controlled according to the experimental requirement. The electrical response of the sensing element is measured using a suitable resistance-measurement circuit/load resistor, in which the change in resistance of the NiS thick film upon exposure to the target gas is converted into a measurable electrical signal. During measurement, the required quantity of test gas is introduced into the 25 L chamber through the gas-inlet port, while the chamber is maintained in a closed condition to obtain the desired gas concentration. The gas molecules diffuse throughout the chamber and come into contact with the active surface of the NiS thick film. Before gas exposure, the sensor is allowed to stabilize in air at the selected operating temperature to establish a stable baseline resistance [19-21]. After introducing the target gas, adsorption of gas molecules on the NiS surface and their interaction with surface-adsorbed oxygen species produce a change in the charge-carrier concentration and consequently alter the electrical resistance of the sensing film. This resistance variation is monitored continuously with time and used to determine the gas response, response time, recovery time and selectivity of the sensor. After completion of the exposure period, the gas is removed through the outlet and the chamber is allowed to return to air conditions, enabling desorption of the adsorbed gas species and recovery of the sensor toward its initial resistance. Different gas concentrations can be obtained by injecting predetermined volumes of the respective test gas into the 25 L chamber; in the present study, concentrations of 200, 400, 600, 800 and 1000 ppm may be obtained by injecting approximately 5, 10, 15, 20 and 25 mL respectively, under the corresponding experimental conditions. The complete arrangement therefore provides a controlled environment for investigating the temperature-dependent and concentration-dependent gas-sensing characteristics of the NiS thick films [20-24].

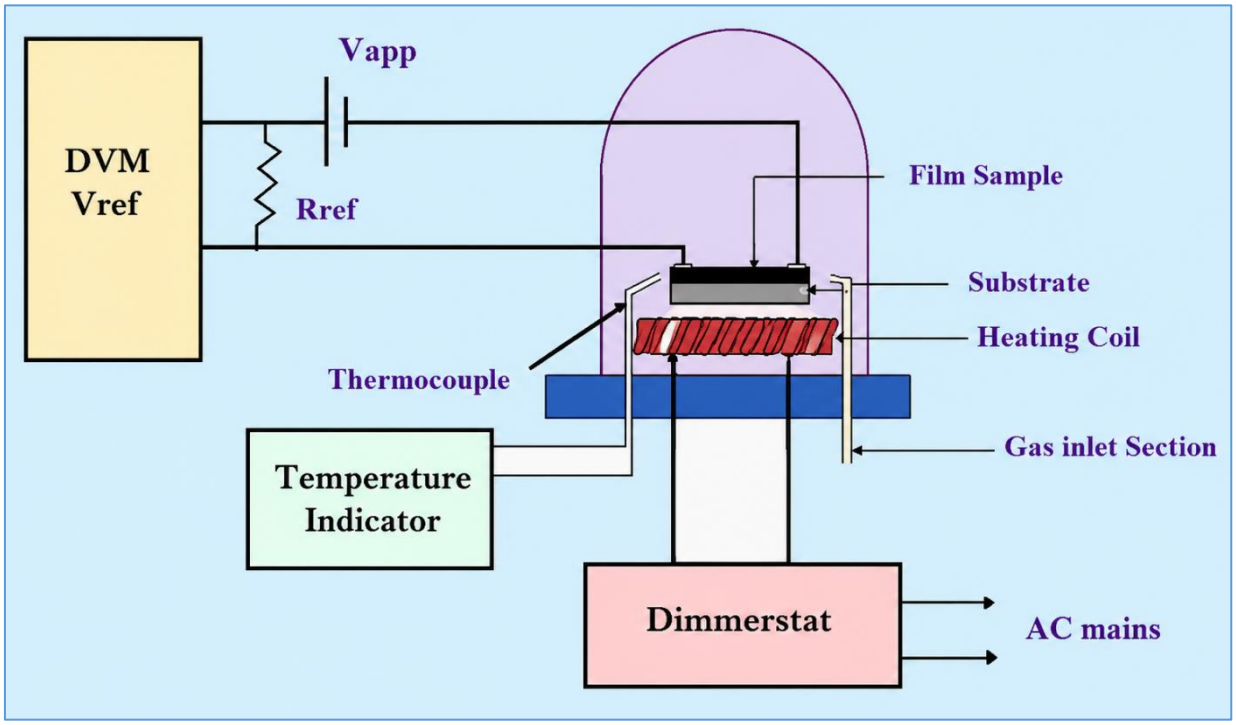

Fig. 1. Schematic diagram of gas sensing system

Figure 2 illustrates the variation in gas response of the screen-printed NiS thick films toward different test gases, namely LPG, NH_3, H_2S, C_2H_5OH (ethanol), NO_2 and CH_4, at operating temperatures of 40, 80, 120, 160 and 200 °C. The gas response of the NiS thick film exhibits a strong dependence on operating temperature, which can be attributed to the temperature-dependent adsorption and desorption of gas molecules and the interaction of these molecules with the chemisorbed oxygen species present on the NiS surface. At 40 °C, the NiS thick film shows relatively low responses of 9.85% for LPG, 3.54% for NH_3, 2.89% for H_2S, 1.64% for ethanol, 5.68% for NO_2 and 1.47% for CH_4, indicating insufficient thermal energy for effective gas adsorption and surface reaction [25, 26]. With an increase in temperature to 80 °C, the response increases considerably for LPG, NH_3, H_2S and ethanol, reaching 23.36%, 12.47%, 8.64% and 5.22% respectively, whereas the NO_2 response decreases slightly to 3.18%. The most pronounced enhancement in LPG sensing is observed at 120 °C, where the response reaches a maximum value of 66.39%, demonstrating that this temperature provides favorable conditions for LPG adsorption, surface reaction and charge-transfer processes on NiS. At the same temperature, the responses toward NH_3, H_2S, ethanol, NO_2 and CH_4 are 23.51%, 11.37%, 25.68%, 41.67% and 6.54% respectively.

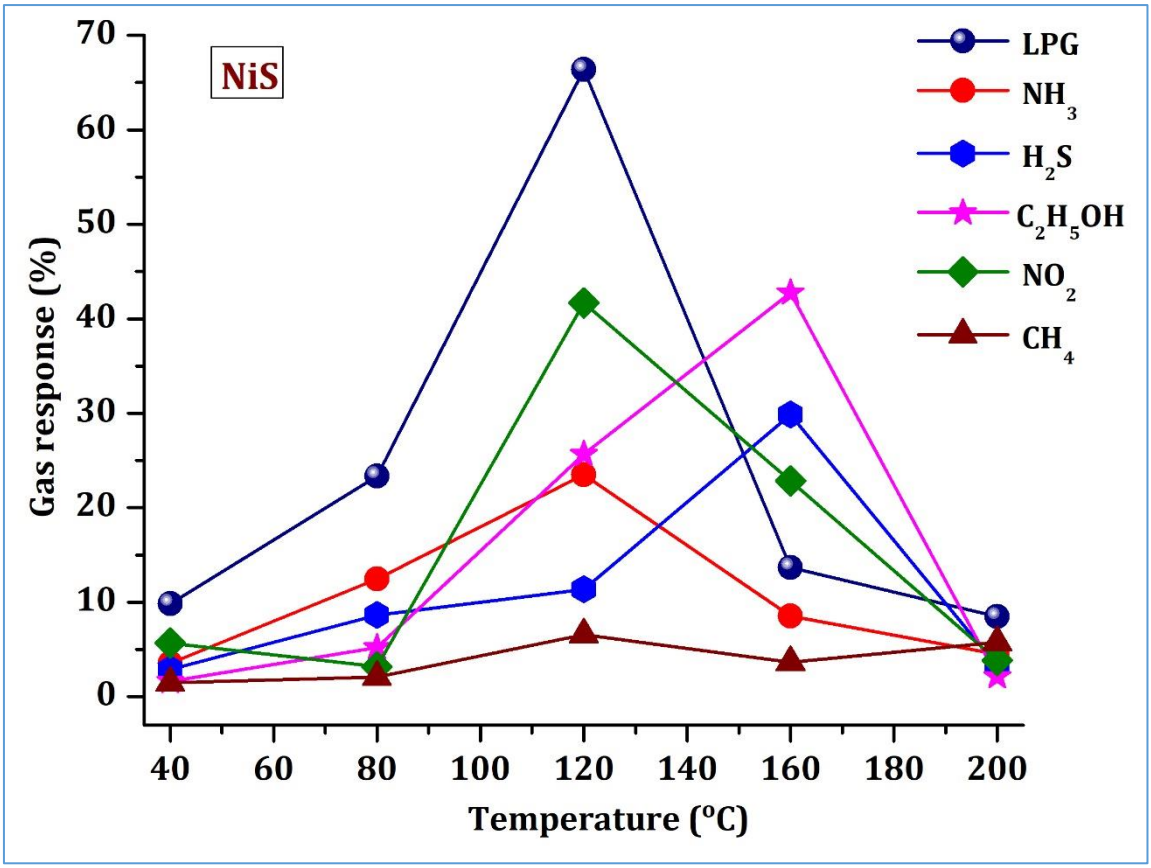

Fig. 2. Gas response versus operating temperature plot of NiS thick films

Thus, 120 °C can be considered the optimum operating temperature for LPG sensing, while the NiS thick film also exhibits appreciable responses toward ethanol and NO_2. Further increasing the operating temperature to 160 °C causes the LPG response to decrease sharply to 13.69%, whereas the responses toward H_2S and ethanol increase substantially to 29.86% and 42.75% respectively. The NO_2 response decreases to 22.84%, while NH_3 and CH_4 show relatively low responses of 8.51% and 3.62%, respectively. The maximum response toward H_2S (29.86%) and ethanol (42.75%) is therefore obtained at 160 °C, suggesting that these gases require a higher activation energy for efficient surface interaction with the NiS film. At 200 °C, the gas responses decrease considerably for all gases, with values of 8.46% for LPG, 4.52% for NH_3, 3.26% for H_2S, 2.11% for

ethanol, 3.84% for NO_2 and 5.74% for CH_4. This reduction at higher temperature may be attributed to enhanced thermal desorption of the adsorbed gas species, which reduces the effective surface coverage and consequently decreases the gas–surface interaction. The temperature-dependent response can generally be explained by the adsorption of oxygen molecules on the NiS surface, followed by electron exchange between adsorbed oxygen species and the target gas molecules [25-28]. Changes in the surface charge density and depletion/accumulation layer modify the electrical resistance of the NiS thick film, producing the observed sensor response

Figure 3 presents the selectivity characteristics of the screen-printed NiS thick film toward different test gases, namely LPG, NH_3, H_2S, C_2H_5OH (ethanol), NO_2 and CH_4. Selectivity is an important parameter for evaluating the ability of a gas-sensing material to preferentially respond to a particular target gas in the presence of other interfering gases. The selectivity values obtained for LPG, NH_3, H_2S, ethanol, NO_2 and CH_4 are 100%, 35.41%, 17.13%, 38.68%, 62.77% and 9.85%, respectively. Among all the investigated gases, the NiS thick film exhibits the highest selectivity toward LPG (100%), indicating a strong preferential interaction between LPG molecules and the NiS sensing surface [23, 24]. The comparatively high selectivity toward NO_2 (62.77%) suggests that NO_2 molecules also interact effectively with the active surface sites of NiS. Moderate selectivity values are observed for ethanol (38.68%) and NH_3 (35.41%), whereas a relatively lower response is obtained for H_2S (17.13%) and CH_4 (9.85%). The superior LPG selectivity can be attributed to the favorable adsorption and surface reaction of LPG molecules with chemisorbed oxygen species on the NiS surface, resulting in a significant modification of the surface charge carrier concentration and consequently a larger change in electrical resistance. The porous and active surface of the thick film may provide numerous adsorption sites, facilitating gas–surface interaction and enhancing the sensing response. In contrast, the lower selectivity toward CH_4 and H_2S indicates relatively weaker interaction or less efficient charge-transfer processes at the NiS surface under the selected operating conditions [23-26].

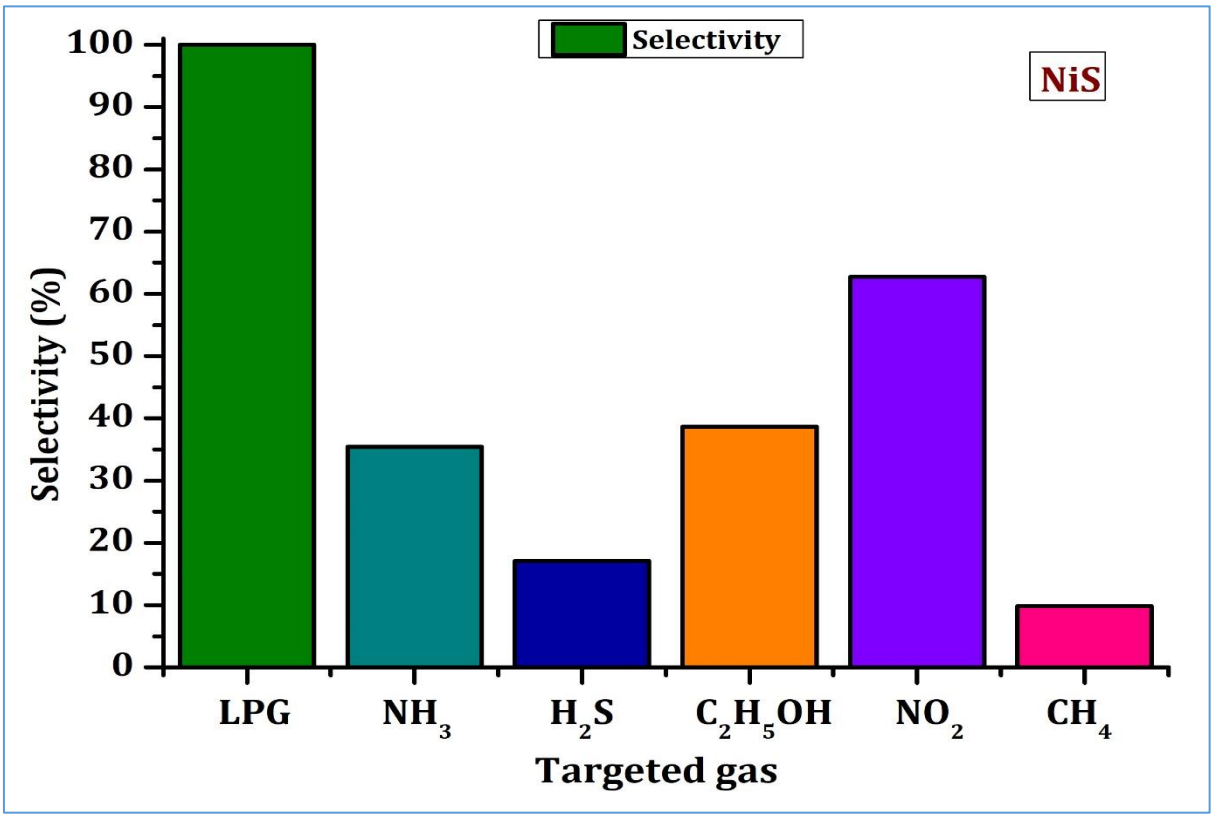

Fig. 3. Selectivity histogram plot of NiS thick films

Figure 4 shows the variation in gas response of the screen-printed NiS thick film with increasing LPG concentration in the range of 100–1000 ppm. The gas response is strongly dependent on LPG concentration, indicating effective interaction between LPG molecules and the active sensing sites present on the NiS surface. At 100 ppm, the NiS thick film exhibits a gas response of 46.58%, which increases to 51.23% at 300 ppm. A further increase in LPG concentration to 500 ppm results in a maximum gas response of 66.39%. This enhancement can be attributed to the increasing number of LPG molecules reaching and interacting with the active sites of the NiS surface, resulting in enhanced surface reaction and charge transfer [26, 27]. The maximum response of 66.39% at 500 ppm suggests that this concentration provides favorable conditions for LPG adsorption and the associated electrical resistance change of the NiS thick film. However, when the LPG concentration is increased further to 700 ppm, the gas response decreases to 53.24%. This reduction may be associated with the saturation of active adsorption sites on the NiS surface, which limits further effective interaction between the gas molecules and the sensing material [27, 28]. At 1000 ppm, the response increases again to 61.75%, indicating continued interaction of LPG molecules with the NiS surface at higher concentration, although the response remains slightly lower than the maximum value obtained at 500 ppm.

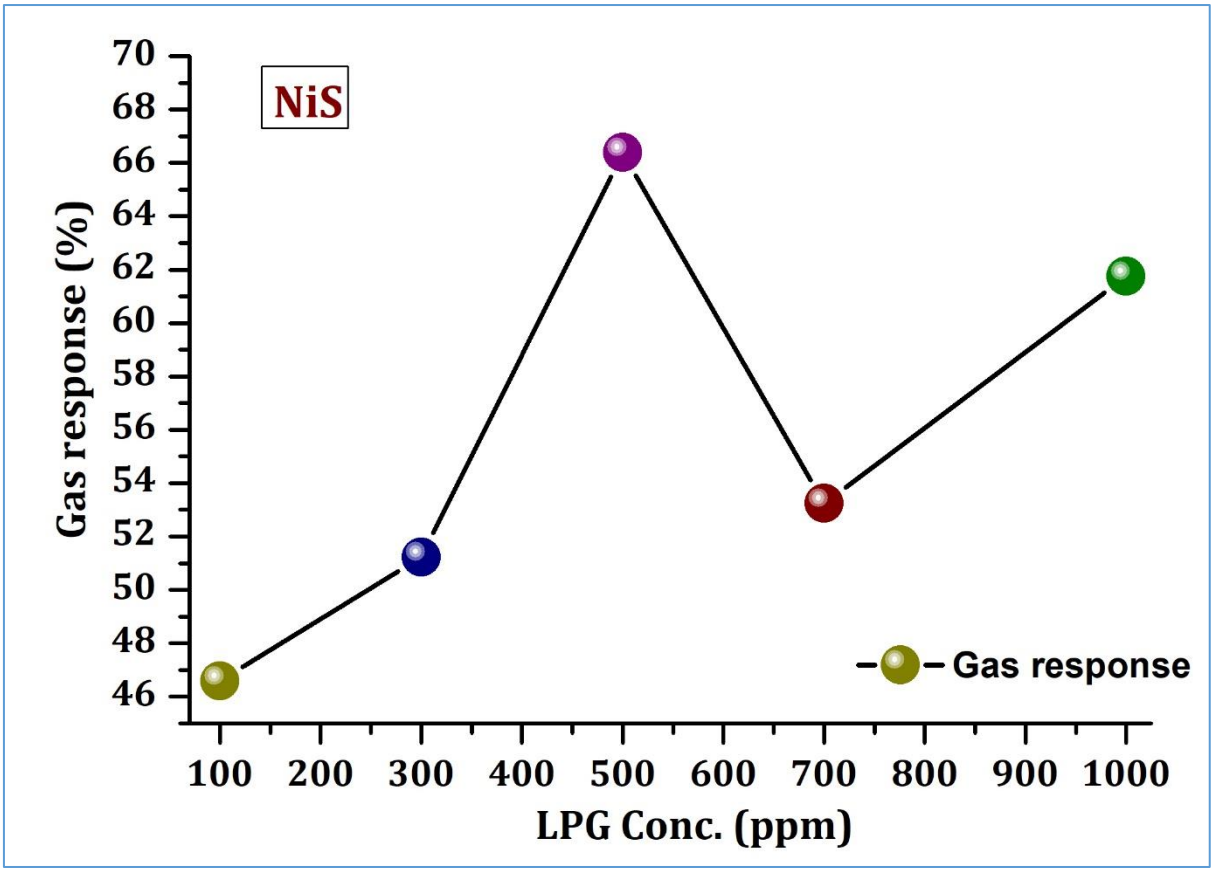

Fig. 4. Gas response versus LPG gas concentration plot of NiS thick films

The overall variation in response can be explained by the adsorption–desorption equilibrium of LPG molecules and the availability of surface-active sites. The NiS thick film provides an active surface where adsorbed oxygen species participate in surface reactions with LPG molecules, producing a change in the concentration of charge carriers and consequently modifying the electrical resistance of the sensing layer. Therefore, the observed maximum response of 66.39% at 500 ppm LPG demonstrates the promising LPG sensing capability of screen-printed NiS thick films [28, 29]. The results indicate that NiS is a potential sensing material for LPG detection and monitoring applications, particularly around the optimized concentration and operating temperature conditions [30, 31].

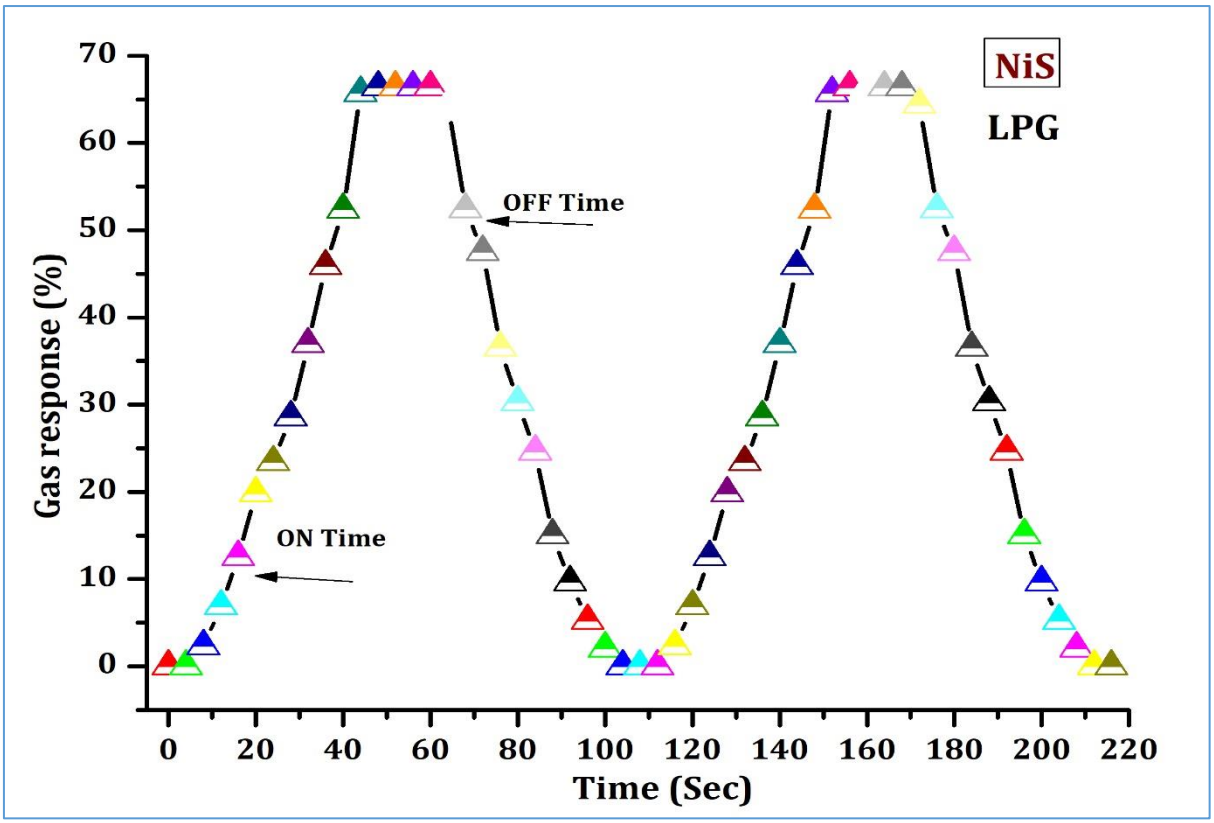

Fig. 5. Response and recovery plot of NiS thick films

Figure 5 illustrates the response and recovery characteristics of the screen-printed NiS thick film toward LPG gas. The sensing response was evaluated as a function of time under repeated ON–OFF gas exposure cycles. When LPG is introduced into the sensing chamber, the gas molecules interact with the adsorbed oxygen species and active surface sites of the NiS thick film, producing a rapid change in the electrical resistance and consequently an increase in the sensor response. The response increases progressively from the baseline and reaches approximately 66%, indicating effective interaction between LPG molecules and the NiS sensing surface [24, 26]. The response time is approximately 23 s, defined as the time required for the sensor to reach about 90% of its maximum response after exposure to LPG. This relatively short response time indicates rapid adsorption and charge-transfer processes at the NiS surface. When the LPG supply is switched OFF and the sensor is exposed to air, the adsorbed gas species gradually desorb from the sensing surface, causing the sensor response to return toward its initial baseline value [8, 9]. The corresponding recovery time is approximately 78 s, indicating that desorption and restoration of the original surface condition require a comparatively longer period than the adsorption process. The repeated response–recovery cycles shown in Fig. 5 demonstrate that the NiS thick film can undergo reversible interaction with LPG and return toward its baseline after removal of the gas [11, 28]. The difference between the response and recovery times can be attributed to the kinetics of gas adsorption, surface reaction, desorption and diffusion of gas molecules through the thick-film sensing layer. The reasonably fast response together with reproducible recovery behavior confirms the suitability of screen-printed NiS thick films for LPG sensing applications [31, 32]. The observed 23 s response time and 78 s recovery time indicate that the NiS thick film possesses favorable dynamic sensing characteristics and can be considered a promising material for the development of LPG gas sensors.

Conclusions

1. NiS nanoparticles were successfully synthesized by the chemical precipitation method and subsequently used for the fabrication of NiS thick films by the screen-printing technique.

2. The screen-printing technique provided a simple, economical and reproducible method for preparing NiS thick films suitable for gas-sensing measurements.
3. The NiS thick film exhibited a temperature-dependent gas response toward LPG, NH_3, H_2S, C_2H_5OH, NO_2 and CH_4, confirming its sensitivity to different gas species.
4. Among the investigated gases, LPG showed the highest gas response of 66.39% at 120 °C, demonstrating the excellent sensing capability of NiS toward LPG.
5. The NiS thick film exhibited appreciable responses toward NO_2 (41.67% at 120 °C), ethanol (42.75% at 160 °C), H_2S (29.86% at 160 °C), NH_3 (23.51% at 120 °C) and CH_4 (6.54% at 120 °C).
6. The selectivity study revealed a maximum selectivity of 100% toward LPG, followed by NO_2 (62.77%), ethanol (38.68%), NH_3 (35.41%), H_2S (17.13%) and CH_4 (9.85%).
7. The LPG concentration-dependent investigation showed that the response increased from 46.58% at 100 ppm to a maximum of 66.39% at 500 ppm LPG, indicating effective interaction between LPG molecules and the active sites of the NiS surface.
8. At higher LPG concentrations, the variation in response can be attributed to progressive occupation and possible saturation of active adsorption sites on the NiS surface.
9. The dynamic sensing investigation demonstrated a response time of 23 s and recovery time of 78 s, indicating reasonably rapid response and satisfactory recovery characteristics.
10. The gas-sensing mechanism can be attributed mainly to adsorption–desorption processes and charge-transfer interactions between LPG molecules, chemisorbed oxygen species and the NiS sensing surface, resulting in measurable changes in electrical resistance.
11. The combination of high LPG response, excellent LPG selectivity and satisfactory response/recovery characteristics confirms the potential of NiS thick films for practical gas-sensing applications.

Acknowledgment

The author would like to express their sincere gratitude to the Principal, Karmaveer Ramraoji Aher Arts, Science and Commerce College, Deola, Tal. Deola, Dist. Nashik, Maharashtra, India, for providing the necessary institutional support, laboratory facilities and encouragement to carry out the present research work.

REFERENCES:

1. Karthikeyan, R., Thangaraju, D., Prakash, N. and Hayakawa, Y. (2015) 'Single-step synthesis and catalytic activity of structure-controlled nickel sulfide nanoparticles', CrystEngComm, 17, pp. 8425–8433.
2. Roffey, A., Hollingsworth, N., Islam, H.-U., Mercy, M., Sankar, G., Catlow, C.R.A., Hogarth, G. and de Leeuw, N.H. (2016) 'Phase control during the synthesis of nickel sulfide nanoparticles from dithiocarbamate precursors', Nanoscale, 8, pp. 11067–11075.
3. Fazli, Y., Pourmortazavi, S.M., Kohsari, I. and Karimi, M.S. (2016) 'Synthesis, characterization and photocatalytic property of nickel sulfide nanoparticles', Journal of Materials Science: Materials in Electronics, 27, pp. 6900–6908.
4. Huang, X.-Y., Chi, Z.-T., Liu, J., Li, D.-H., Sun, X.-J., Yan, C., Wang, Y.-C., Li, H., Wang, X.-D. and Xie, W.-F. (2020) 'Enhanced gas sensing performance based on p-NiS/n-In_2O_3 heterojunction nanocomposites', Sensors and Actuators B: Chemical, 304, 127305.
5. Wagh, R.V., Yewale, C.R., Deshmane, V.V., Tupe, U.J., Mandawade, S.S., Naeem, S. and Patil, A.V. (2025) 'Exploring spray pyrolysis deposited NiS thin films as promising materials for photoactivated gas sensor', Total Chemistry, article 100023.
6. Wang, C., Yin, L., Zhang, L., Xiang, D. and Gao, R. (2010) 'Metal oxide gas sensors: Sensitivity and influencing factors', Sensors, 10(3), pp. 2088–2106.

7. Korotcenkov, G. (2007) 'Metal oxides for solid-state gas sensors: What determines our choice?', Materials Science and Engineering: B, 139(1), pp. 1–23.
8. Shajudheen, M.V.P., Kumar, V.S., Rani, K.A., Maheswari, U.A. and Kumar, S.S. (2016) 'Structural and optical properties of NiS nanoparticles synthesized by chemical precipitation method', International Journal of Innovative Research in Science, Engineering and Technology, 5(8), pp. 15099–15104.
9. Molla, A., Sahu, M. and Hussain, S. (2016) 'Synthesis of tunable band gap semiconductor nickel sulphide nanoparticles: Rapid and round the clock degradation of organic dyes', Scientific Reports, 6, 26034.
10. Barsan, N., Koziej, D. and Weimar, U. (2007) 'Metal oxide-based gas sensor research: How to?', Sensors and Actuators B: Chemical, 121(1), pp. 18–35.
11. Korotcenkov, G. (2008) 'The role of morphology and crystallographic structure of metal oxides in response of conductometric-type gas sensors', Materials Science and Engineering: R: Reports, 61(1–6), pp. 1–39.
12. Batzill, M. (2006) 'Surface science studies of gas sensing materials: SnO_2', Sensors, 6(10), pp. 1345–1366.
13. Comini, E. (2006) 'Metal oxide nano-crystals for gas sensing', Analytica Chimica Acta, 568(1–2), pp. 28–40.
14. Comini, E. (2016) 'Metal oxide nanowire chemical sensors: Innovation and quality of life', Materials Today, 19(10), pp. 559–567.
15. Dey, A. (2018) 'Semiconductor metal oxide gas sensors: A review', Materials Science and Engineering: B, 229, pp. 206–217.
16. Das, S. and Jayaraman, V. (2014) 'SnO_2: A comprehensive review on structures and gas sensors', Progress in Materials Science, 66, pp. 112–255.
17. Moseley, P.T. (1992) 'Materials selection for semiconductor gas sensors', Sensors and Actuators B: Chemical, 6(1–3), pp. 149–156.
18. Yamazoe, N. and Shimanoe, K. (2013) 'Fundamentals of semiconductor gas sensors', in Semiconductor Gas Sensors. Elsevier, pp. 3–34.
19. Yamazoe, N. and Shimanoe, K. (2008) 'Theory of power laws for semiconductor gas sensors', Sensors and Actuators B: Chemical, 128(2), pp. 566–573.
20. Ménil, F., Lucat, C. and Debéda, H. (1995) 'The thick-film route to selective gas sensors', Sensors and Actuators B: Chemical, 25(1–3), pp. 415–420.
21. Vincenzi, D., Butturi, M.A., Stefancich, M., Malagù, C., Guidi, V., Carotta, M.C., Martinelli, G., Guarnieri, V., Brida, S., Margesin, B., Giacomozzi, F., Zen, M., Vasiliev, A.A. and Pisliakov, A.V. (2001) 'Low-power thick-film gas sensor obtained by a combination of screen printing and micromachining techniques', Thin Solid Films, 391(2), pp. 288–292.
22. Vincenzi, D., Butturi, M.A., Guidi, V., Carotta, M.C., Martinelli, G., Guarnieri, V., Brida, S., Margesin, B., Giacomozzi, F., Zen, M., Pignatel, G.U., Vasiliev, A.A. and Pisliakov, A.V. (2001) 'Development of a low-power thick-film gas sensor deposited by screen-printing technique onto a micromachined hotplate', Sensors and Actuators B: Chemical, 77(1–2), pp. 95–99.
23. Montanaro, L. and Tersalvi, A. (2000) 'Set up of a screen-printing procedure for the production of a beta alumina-based gas sensor', Journal of Electroceramics, 5(3), pp. 253–259.
24. Feng, L.-D., Huang, X.-J. and Choi, Y.-K. (2006) 'Dynamic determination of domestic liquefied petroleum gas down to several ppm levels using a Sr-doped SnO_2 thick film gas sensor', Microchimica Acta, 156(3–4), pp. 245–251.

25. Dighavkar, C.G., Patil, A.V. and Borse, R.Y. (2009) 'Study on gas sensing performance of TiO_2 screen printed thick films', Sensors & Transducers Journal, 101(2), pp. 73–81.
26. Khadayate, R.S. and Patil, P.P. (2010) 'CO gas sensing properties of screen printed SnO_2 thick films', Journal of Optoelectronics and Advanced Materials, 12(6), pp. 1338–1342.
27. Patil, A.V., Dighavkar, C.G., Sonawane, S.K., Patil, S.J. and Borse, R.Y. (2010) 'Formulation and characterization of Cu doped ZnO thick films as LPG gas sensor', Sensors & Transducers, 9(Special Issue), pp. 11–20.
28. Yadav, B.C., Singh, S. and Yadav, A. (2011) 'Nanonails structured ferric oxide thick film as room temperature liquefied petroleum gas (LPG) sensor', Applied Surface Science, 257(6), pp. 1960–1966.
29. Srivastava, R. (2014) 'Nanocomposite $ZnNb_2O_6$ thick film as room temperature liquefied petroleum gas (LPG) sensor', American Journal of Sensor Technology, 2(2), pp. 25–28.
30. Janata, J. (2009) Principles of Chemical Sensors. New York: Springer.
31. Ferroni, M., Guidi, V., Martinelli, G., Faglia, G., Sberveglieri, G. and Nelli, P. (1996) 'Characterization of a gas sensor based on a nanostructured titania thick film', Nanostructured Materials, 7(7), pp. 709–716.
32. Ushir, V.J., Baste, Y.R., Uphade, B.K. and Ghotekar, J.N. (2026) 'Facile synthesis and characterization of NiS and Co-doped NiS nanomaterials for photocatalytic and gas sensing applications', Topics in Catalysis. This recent study is particularly relevant because it reports NiS and Co-doped NiS nanomaterials prepared by co-precipitation for gas-sensing applications